

A DETAILED ANALYSIS OF MULTI-SENSOR FUSION OF MODERATE RESOLUTION IMAGING SPECTRORADIOMETER

Harish Kumar¹, Hussein Yahia¹ and Singh D²

¹Geo-Stat team, INRIA Bordeaux Sud-Ouest, 351 Cours de La Liberation, 33405 Talence Cedex, France.
phone: + 33 524574049, fax: +33 524574124, email: (harish-kumar, hussein.yahia)@inria.fr.

²Department of Electronics and Computer Engg, Indian Institute of Technology Roorkee, India. email: dharmfec@gmail.com.

ABSTRACT

The main aim of this paper is to develop a monitoring system for the analysis of Land cover classes (Agriculture, Urban and water). Hence in this perspective, the use of Moderate Resolution Imaging Spectroradiometer (MODIS) Satellite data is a good choice, as because of its temporal as well as spectral capability and as well as it is freely available. The problems with MODIS data are their poor spatial resolution. This problem can be minimized by application of the fusion techniques where high resolution data will be used to fuse with low resolution data. Hence in this paper, we have considered to fuse, high resolution i.e., like 15m resolution Advanced Spaceborne Thermal Emission and Reflection Radiometer (ASTER) data with moderate resolution i.e., like 250m Terra MODIS satellite data. The main aim of this paper is to analyze the effect of classification accuracy on major type of land cover types like agriculture, water and urban bodies with fusion of ASTER data to MODIS data. Curvelet transformation has been applied for fusion of these two satellite data and Minimum Distance classification technique has been applied for the resultant fused data. It is quantitatively observed that the overall classification accuracy of MODIS data after fusion is quite enhanced. This type of fusion technique may be quite helpful in near future to maximize the use of freely available satellite data and consequently to develop a monitoring system

1. INTRODUCTION

Since, the launch of the first Earth resource satellite, i.e., Landsat-1 in 1972, satellite data processing has become an increasingly important tool for the inventory, monitoring, management of earth resources and many other applications [1]. The increasing availability of information products generated from satellite data has added greatly to our ability to understand the patterns and dynamics of the earth resource systems at all scales of inquiry [2, 3]. In which one of the most important application is the generation of land cover classification from satellite data for understanding the actual status of various classes. Compared to more traditional mapping approaches such as terrestrial survey and basic aerial photo interpretation, land-use mapping using satellite data has the advantages of low cost, large area coverage, repetitively, and computability.

The prospect for the use of satellite data in land cover classification is an extremely promising one. The availability of moderate resolution imaging Spectroradiometer (MODIS) data with greatly improved spectral, spatial, geometric, and radiometric attributes provides significant new opportunities and challenges for remote sensing-based land cover classi-

fication [4]. But, maximum high resolution satellite data is high priced and it is need of research to explore the maximum utilization of freely available satellite data. For the full exploitation of increasingly sophisticated multisource data, fusion techniques are being developed. It is the aim of image fusion to integrate different data in order to obtain more information that can be derived from each of the single sensor data alone. The fusion of these disparate data contributes to the increasing classification accuracy as stated by [5].

Many image fusion methods have been proposed, a detailed review on this issue was given by [5]. Some methods such as intensity-hue-saturation (IHS)[6, 7], Brovey transform [8, 9] and principal component analysis [9, 10] provide superior visual high-resolution multispectral images, but have a limitation of high-quality spectral information, while these methods are useful for visual interpretation. High-quality spectral information is very important for most remote sensing applications based such as land cover classification [11]. The high-quality synthesis of spectral information is particularly well suited in the case of land cover classification was implied by [12]. More recently, an underlying multiresolution analysis employing the discrete wavelet transform has been used in image fusion. It was found that multisensor image fusion is a tradeoff between the spectral information from a low resolution Multispectral Images and the spatial information from a high resolution multispectral Images. With the wavelet transform fusion method, it is easy to control this tradeoff [13].

The wavelet-transform fusion method provides a high spectral quality in fused satellite data. However, data fused by wavelets have much less spatial information than those fused by the intensity-hue-saturation, Brovey transform, principal component analysis [14, 15]. For Land cover classification, the spatial information of a fused data is just as important as the spectral information. Therefore, there is a need to develop an advanced method of image fusion, so that fused data have the same spectral resolution as MODIS data and the spatial resolution as ASTER data.

In recent Years [16] has used a new transform, the curvelet transform. The curvelet transform is obtained by applying the Ridgelet transform [17] to square blocks of detail frames of undecimated wavelet decomposition. Since the Ridgelet transform possesses basis functions matching directional straight lines, the curvelet transform is capable of representing piecewise linear contours on multiple scales through few significant coefficients. This property leads to a better separation between geometric details and background noise, which may be easily reduced by thresholding curvelet coefficients before they are used for fusion [16]. Hence the curvelet transform, therefore, represents edges better than

wavelets and is well suited for extracting detailed spatial information, as well as spectral information from an image, and hence, can be very useful for clustering the various targets.

The Terra and Aqua Moderate Resolution Imaging Spectroradiometer (MODIS) [18] instrument provides high radiometric sensitivity (12 bit) in 36 spectral bands ranging in wavelength from 0.4 μm to 14.4 μm and also it is freely available. In this paper, the band 1 of spatial resolution 250 m and bandwidth 620-670 nm, and band 2, of spatial resolution of 250m and bandwidth 842-876 nm is considered as these bands has special features to identify the agriculture and other land covers.

The Advanced Spaceborne Thermal Emission and Reflection Radiometer (ASTER) [19] is a high spatial resolution multi-spectral imaging radiometer, and is onboard the NASA's Terra spacecraft. In this paper, Band 2 with a resolution of 15m and bandwidth 630 to 690 nm is considered and Band 3 with a resolution of 15m and bandwidth 760 to 860 nm is considered as these bands bandwidth are quite near to the MODIS bands which we have selected for analysis.

The MODIS data are freely and easily available whereas ASTER data has to be purchased. Another important aspect of MODIS data is that it is highly temporal (i.e., data is available in a couple of days). Therefore, the MODIS data may also be very useful for time series analysis, which is the one of the requirement for developing a monitoring system. The spatial resolution of ASTER data is 15m to 90m while as the spatial resolution of MODIS data is 250m to 1000m. Hence in this paper, the ASTER data is fused with the MODIS data. There is a need of research to explore the possibility of use of MODIS data for land cover enhancement with fusion techniques. Therefore, in this paper, we have attempted to explore the effect of fusion of MODIS and ASTER data on land cover enhancement.

2. STUDY AREA

Roorkee Region is selected as the study. The area is relatively flat with a maximum slope of 4° (elevations ranging from 245.5 m to 289.9 m above the sea level). The region extends from 29°77' N and 30° N, and its longitude ranges from 77°83' E and 78°01' E. The study area basically consists of agricultural, water and urban classes. Urban class is mostly comprised of residential areas.

2.1 Data Used

- ASTER data of Level 1B is used which is taken on 17th March 2001
- The MODIS image considered is MODIS/Terra Surface Reflectance 8-Day L3 Global 250m SIN Grid of March 22, 2001.

Both satellite data covers approximate the same spectral range.

3. THEORETICAL BASIS

3.1 Curvelet Transform for Fusion

In this paper curvelet fusion is applied to fuse high resolution ASTER data on moderate resolution MODIS data. The main feature of the curvelet transform is that it is sensitive to directional edges and capable of representing the high-pass details of object contours at different scales through few sparse nonzero coefficients. In the subsequent section,

the ATrous wavelet transform, which represents the starting point of the curvelet transform is reviewed, the ridgelet transform by which the curvelet transform is derived, is introduced, then the curvelet transform is briefly outlined.

3.2 A Trouw Wavelet Transform

The ATrous wavelet transform (ATWT) [20] is a nonorthogonal multiresolution decomposition defined by a filter bank $\{h_n\}$ and $\{g_n=\delta_n-h_n\}$, with the Kronecker operator δ_n denoting an allpass filter. The filter bank does not allow perfect reconstruction to be achieved if the output is decimated. In the absence of decimation, the lowpass filter is upsampled by 2^j , before processing the j^{th} level. Hence the name ATrous which means with holes.

For J-level decomposition, the ATWT accommodates a number of coefficients J + 1 time greater than the number of pixels. Due to the absence of decimation, the synthesis is simply obtained by summing details levels to the approximation:

$$f(m,n) = c_J(m,n) + \sum_{j=1}^J d_j(m,n) \quad (1)$$

Where $c_j(m,n)$ and $d_j(m,n)$, $j = 1, \dots, J$ are obtained through 2-D separable linear convolution with the equivalent lowpass and highpass filters, respectively.

3.3 Ridgelet Transform

The next step is finding a transformation capable of representing straight edges with different slopes and orientations. A possible solution is the ridgelet transform [17], which may be interpreted as the 1-D wavelet transform of the Radon transform. The ridgelet basis function is given by [21, 22]:

$$\Psi_{a,b,\theta}(x_1,x_2) = a^{-\frac{1}{2}} \psi\left(\frac{x_1 \cos \theta + x_2 \sin \theta - b}{a}\right) \quad (2)$$

for each $a>0$, each $b \in \mathbb{R}$ and each $\theta \in [0, 2\pi)$. This function is constant along lines $x_1 \cos \theta + x_2 \sin \theta = \text{const}$. Thus, the ridgelet coefficients of an data $f(x_1, x_2)$, are represented by

$$R_f(a,b,\theta) = \int_{-\infty}^{\infty} \int_{-\infty}^{\infty} \Psi_{a,b,\theta}(x_1,x_2) f(x_1,x_2) dx_1 dx_2 \quad (3)$$

This transform is invertible and the reconstruction formula is given by:

$$f(x_1,x_2) = \int_0^{2\pi} \int_{-\infty}^{\infty} \int_0^{\infty} R_f(a,b,\theta) \Psi_{a,b,\theta}(x_1,x_2) \frac{da}{a^3} db \frac{d\theta}{4} \quad (4)$$

The Radon transform for an object f is the collection of line integrals indexed by $\theta \in [0, 2\pi) * \mathbb{R}$ and is given by:

$$Rf(\theta,t) = \int_{-\infty}^{\infty} \int_{-\infty}^{\infty} f(x_1,x_2) * \delta(x_1 \cos \theta + x_2 \sin \theta - t) dx_1 dx_2 \quad (5)$$

Thus, the ridgelet transform can be represented in terms of the Radon transform as follow:

$$R_f(a,b,\theta) = \int_{-\infty}^{\infty} Rf(\theta,t) a^{-\frac{1}{2}} \psi\left(\frac{t-b}{a}\right) dt \quad (6)$$

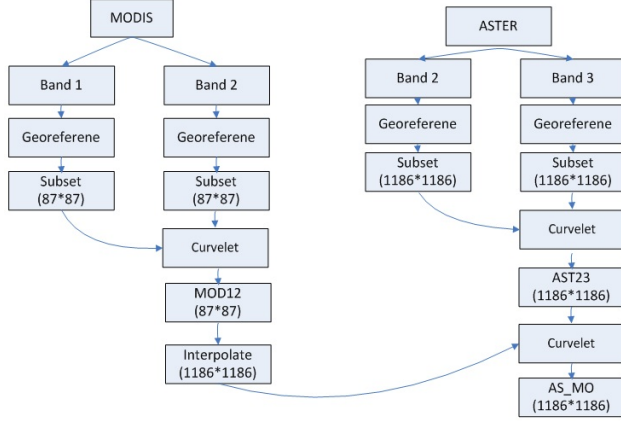


Figure 1: Flowchart indicating the methodology for the fusion of ASTER and MODIS data

Hence, the ridgelet transform is the application of the 1-D wavelet transform on the slices of the Radon transform where the angular variable θ is constant and t is varying.

3.4 Curvelet Transform

The curvelet transform is given by filtering and applying multiscale ridgelet transform on each bandpass filters which is described as following in different steps

3.4.1 Subband Decomposition

The data is filtered into subbands

$$f \rightarrow (P_0 f, \Delta_1 f, \Delta_2 f, \dots) \quad (7)$$

where a filter P_0 deals with frequencies $\xi \leq 1$ and the bandpass filter Δ_s is concentrated near the frequencies $[2^s, 2^{s+2}]$, e.g., $\Delta_s = \psi_{2^s} * f$, $\psi_{2^s}(\xi) = \psi(2^{-2s}\xi)$

3.4.2 Smooth Partitioning

Each subband is smoothly windowed into squares of an appropriate scale.

$$\Delta_s f \rightarrow (w_Q \Delta_s f), Q \in Q_s \quad (8)$$

3.4.3 Renormalization

Each resulting square is renormalized to unit scale.

$$g_Q = (T_Q)^{-1}(w_Q \Delta_s f), Q \in Q_s \quad (9)$$

3.4.4 Ridgelet Analysis

Each square is analyzed via the discrete ridgelet transform.

4. IMPLEMENTATION OF DEVELOPED APPROACH

Figure 1 shows the flowchart of the proposed methodology for the curvelet fusion of ASTER data and MODIS data for analyzing the classification of the MODIS data before and after the fusion. MODIS and ASTER data are subsetted to Roorkee region for this study. After subsetting MODIS has 87*87 pixels and ASTER has 1186*1186 number of pixels, by which both are acquiring approximately the same area. The flowchart fig. 1 is deciphered in the following steps

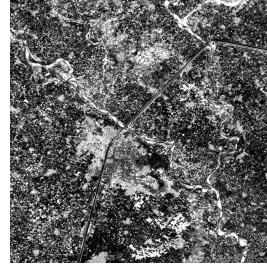


Figure 2: ASTER Band 2

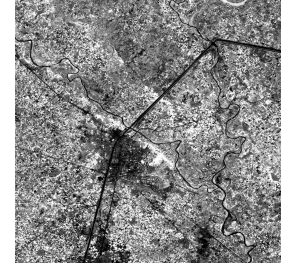


Figure 3: ASTER Band 3



Figure 4: MODIS Band 1

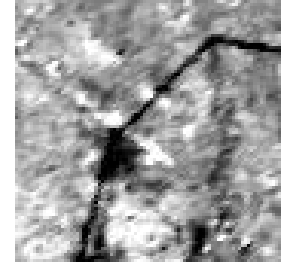


Figure 5: MODIS Band 2

- MODIS Band 1 and Band 2 are considered initially. The Band 1 is fused with the Band 2, through the curvelet transform. (For ATWT transform, equation 1 is computed for Band 2, thereby Band 2 is decomposed into $J + 1$ subbands, which includes C_J & d_j , where C_J is a coarse or smooth version of Band 2, and d_j is the details of Band 2 at scale 2^{-j} , here $j=2$. C_J is replaced by Band 1 and then the Ridgelets transform (equation 2- 6) is applied to all the decomposed subbands i.e. d_j bands, thereby obtained ridgelet coefficients are hard-thresholded in order to enhance edges in the fused data and Inverse Ridgelet transforms (IRT) is carried out to obtain a new data which reflect the fused data of Band 1 and Band 2) Consequently the resultant fused data is MOD12.
- Simultaneously subsetting ASTER data of Band 2 and Band 3 are considered. The Band 2 is fused with the Band 3, through the curvelet transform. Similar fusion process has been applied for fusion of ASTER band 2 and band 3. ATWT transformation is applied for band 3 and C_J is replaced by band 2. Here j is 2. Then ASTER fused data is obtained as AST23.
- The AST23 and MOD12 is the interpolated fused data of MODIS bands are considered for the fusion through curvelet transform. Similar fusion process has been applied for fusion of AST23 and MOD12. ATWT transformation is applied for AST23 and C_J ($j=2$ for present case) is replaced by MOD12 which gives the resultant fused data AS_MO.

5. ANALYSIS OF EXPERIMENTAL RESULTS

The ASTER band 2 and ASTER band 3 which is georeferenced and subset to the Roorkee region is shown in the fig. 2 and 3. MODIS band 1 and MODIS band 2 are shown in fig. 4 and 5 respectively which is georeferenced and subset to the Roorkee region. The Minimum Distance classi-

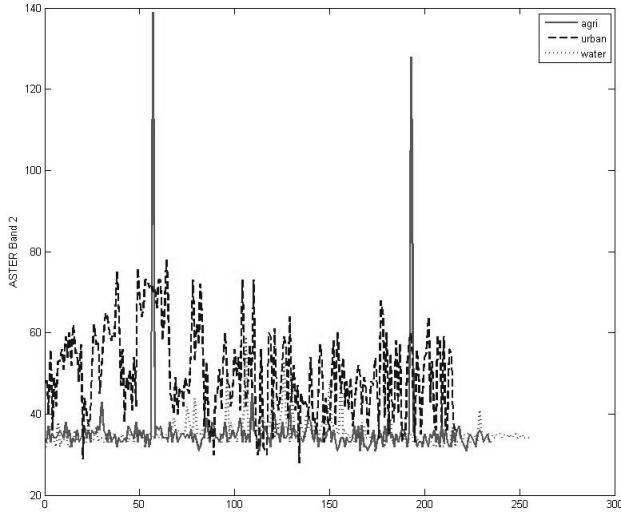


Figure 6: Spectral Response of ASTER Band 2

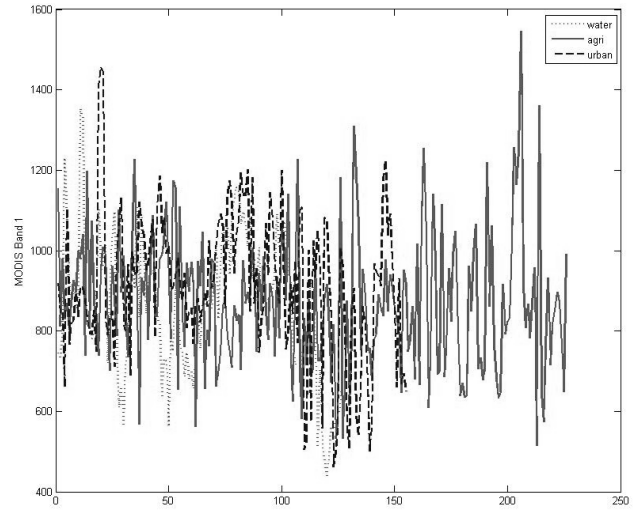


Figure 8: Spectral Response of MODIS Band 1

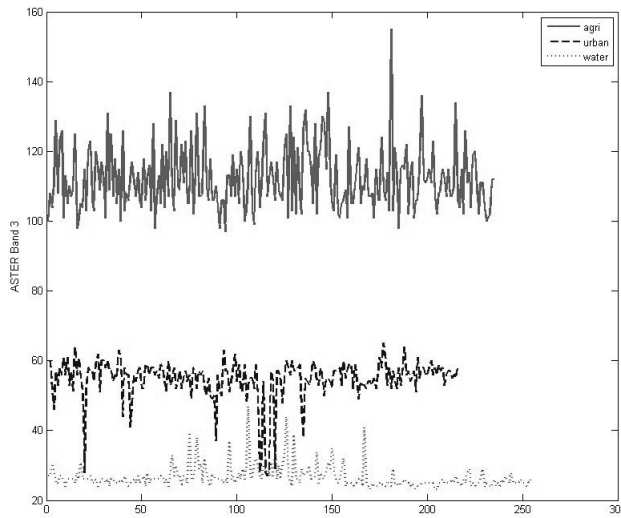


Figure 7: Spectral Response of ASTER Band 3

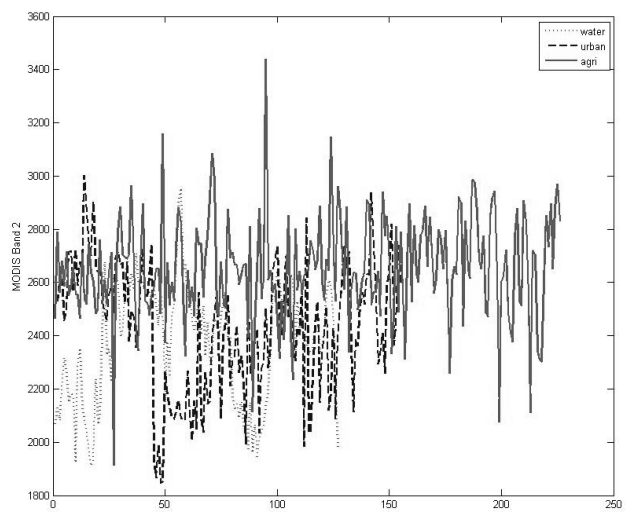


Figure 9: Spectral Response of MODIS Band 2

fication technique has been applied for obtaining the major type of land cover classification i.e. urban, agriculture and water. ENVI 4.3 and MATLAB 7.0 are used for whole processing and algorithm implementation. We have identified 235 Ground Control points (GCP) for agriculture, 216 GCP for urban and 255 GCP for water bodies from Toposheet of Roorkee region, Google earth, and ground survey points. On the basis of these GCPs, we have computed the classification accuracy. The Spectral response for this GCP for ASTER band 2, band 3 and MODIS band 1 and 2 are shown in the fig. 6, 7, 8, 9 respectively (x-axis represents the GCPs considered and y-axis represents the surface reflectance values of corresponding bands).

MODIS band 1 and band 2, ASTER Band 2 and Band 3 are classified by minimum distance classification technique, and thereby the overall classification accuracy is computed and has been tabulated in Table 1. The overall classification accuracy for MODIS band 1, MODIS band 2 is 34.06% and 52.17% respectively. In other hand ASTER band 2, ASTER band 3 has overall accuracy of 72.02% and 98.73% respec-

tively. It is clear from fig. 7 that GCPs have a distinct spectral response for agriculture, urban and water bodies. Hence the classification accuracy is good for ASTER band 3, whereas the same GCPs in ASTER Band 2 (fig. 6) have some overlap spectral response, and hence there is a reduction in the accuracy. In another hand, the spectral response of MODIS Band 1 and MODIS Band 2 (Fig. 8, 9), represents no clear distinction of different land cover. This may be one of the main reasons for having poor classification accuracy for MODIS band 1 and band 2.

Minimum distance classification technique is applied on the resultant fused image of MODIS bands i.e., MOD12, ASTER bands i.e., AST23 and AS_MO (fused image of AST23 and MOD12), and corresponding classification accuracy is computed and tabulated in table 1. It is observed that the resultant fused data i.e., AS_MO has better accuracy than the MODIS data of band 1 and 2. It is also observed that the fused data has enhanced the classification accuracy in comparison to MODIS band 1 data where as with MODIS band 2 it is moderately enhanced the classification accuracy.

Table 1: Classification Accuracy

Data	Producer's Accuracy			Classification Accuracy (%)
	Agriculture	Urban	Water	
ASTER Band 2	27.23	68.06	80.94	72.02
ASTER Band 3	99.67	95.83	98.98	98.73
MODIS Band 1	9.29	56.13	51.18	34.06
MODIS Band 2	73.89	23.87	48.03	52.17
MOD12	54.42	6.45	59.84	41.14
AST23	99.74	95.37	98.82	98.17
AS_MO	82.13	29.17	54.12	54.81

Overall as well as individual classification of each considered land cover has enhanced in the fused data.

6. CONCLUSIONS

A methodology for the enhancement of overall classification accuracy for the MODIS data is presented. The high resolution data (i.e., ASTER) is fused with low or moderate resolution data (i.e., MODIS) and the resultant fused data is analyzed in the viewpoint of land cover classification through the curvelet based fusion. The overall classification accuracy for the fused data is better than the MODIS band 1 and MODIS band 2. This type of fusion may be helpful in near future to maximize the use of MODIS data, and thereby paving the way for developing a land cover monitoring system with MODIS satellite data.

REFERENCES

- [1] Draeger W. C., Holm T. M., Lauer D. T. and Thompson R. J., "The availability of Landsat data: Past, present, and future," *Photogrammetric Engineering and Remote Sensing*, vol. 63, pp. 869–875, 1997.
- [2] Lambin E. F., et al., "The causes of land use and land cover change: Moving beyond the myths," *Global Environment Change*, vol. 11, pp. 261–269, 2001.
- [3] Goldewijk K. K. and Ramankutty N., "Land cover change over the last three centuries due to human activities: the availability of new global data sets," *GeoJournal*, vol. 61, pp. 335–344, 2004.
- [4] Friedl M.A., et al., "Global land cover mapping from MODIS: algorithms and early results," *Remote Sensing of Environment*, vol. 83, pp. 287–302, 2002.
- [5] Pohl C., van Genderen J.L., "Multisensor image fusion in remote sensing: concepts, methods, and applications," *International Journal of Remote Sensing*, vol. 19, 5, pp. 823–854, 1998.
- [6] Edwards K. and Davis P. A., "The use of Intensity-Hue-Saturation transformation for producing color shaded-relief images," *Photogrammetric Engineering and Remote Sensing*, vol. 60, no. 11, pp. 1369–1374, 1994.
- [7] Schetselaar E. M., "Fusion by the IHS transform: Should we use cylindrical or spherical coordinates?," *International Journal of Remote Sensing*, vol. 19, no. 4, pp. 759–765, 1998.
- [8] Gillespie A. R., Kahle A. B., and Walker R. E., "Color enhancement of highly correlated images II. Channel ratio and chromaticity transformation techniques," *Remote Sensing of Environment*, vol. 22, pp. 343–365, 1987.
- [9] Zhou J., Civco D. L. and Silander J. A., "A wavelet transform method to merge Landsat TM and SPOT panchromatic data," *International Journal of Remote Sensing*, vol. 19, no. 4, pp. 743–757, 1998.
- [10] Chavez P. S. and Kwarteng A. Y., "Extracting spectral contrast in Landsat Thematic Mapper image data using selective principle component analysis," *Photogrammetric Engineering and Remote Sensing*, vol. 55, no. 3, pp. 339–348, 1989.
- [11] Liu J. G., "Smoothing filter-based intensity modulation: A spectral preserve image fusion technique for improving spatial details," *International Journal of Remote Sensing*, vol. 21, no. 18, pp. 3461–472, 2000.
- [12] Garguet-Duport B., et al., "The use of multi-resolution analysis and wavelets transform for merging SPOT panchromatic and multi-spectral image data," *Photogrammetric Engineering and Remote Sensing*, vol. 62, no. 9, pp. 1057–1066, 1996.
- [13] Gonzalo Pajares and Jesus Manuel de la Cruz, "A wavelet-based image fusion tutorial," *Pattern Recognition*, vol. 37, pp. 1855–1872, 2004.
- [14] Yocky D.A., "Artifacts in wavelet image merging," *Optical Engineering*, vol. 35 (7), pp. 2094–2101, 1996.
- [15] Gonzales Audcana M., et al., "Fusion of multispectral and panchromatic images using improved IHS and PCA mergers based on wavelet decomposition," *IEEE Transactions on Geoscience and Remote Sensing*, vol. 42 (6), pp. 1291–1299, 2004.
- [16] Starck J. L., Candès E. J. and Donoho D. L., "The curvelet transform for image denoising," *IEEE Transactions on Image Processing*, vol. 11, pp. 670–684, 2002.
- [17] Do M.N., Vetterli M., "The finite ridgelet transform for image representation," *IEEE Transactions on Image Processing*, vol. 12 (1), pp. 16–28, 2003.
- [18] Justice C. O., et al., "The Moderate Resolution Imaging Spectroradiometer (MODIS): land remote sensing for global change research," *IEEE Transactions on Geosciences and Remote Sensing*, vol. 36, pp. 1228–1249, 1998.
- [19] ABRAMS M., "The Advanced Spaceborne Thermal Emission and Reflection Radiometer (ASTER) : data products for the high spatial resolution imager on NASA's Terra platform," *International Journal of Remote Sensing*, vol. 21, no. 5, pp. 847–859, 2000.
- [20] Shensa M.J., "The discrete wavelet transform: wedding the a trous and Mallat algorithm," *IEEE Transactions on Signal Processing*, vol. 40, no. 10, pp. 2464–2482, 1992.
- [21] Filippo Nencini, et al., "Remote sensing image fusion using the curvelet transform," *Information Fusion*, vol. 8, pp. 143–156, 2007.
- [22] Choi M., et al., "Fusion of multispectral and panchromatic satellite images using the curvelet transform," *IEEE Geosciences and Remote Sensing Letters*, Vol. 2, No. 2, pp. 136–140, 2005.